

# Numerical Simulation of Charging Characteristics under the Influence of Photoreceptor Defects

*Satoshi Hasebe and Nobuyuki Nakayama*

*Fuji Xerox Co., Ltd., Document Products Company, R&D Center  
Nakai, Kanagawa, Japan*

## Abstract

Two-dimensional numerical study was carried out on the problem in charging known as the pin-hole leak phenomenon caused by photoreceptor defects in the roller charging system under constant current control with the DC voltage superposed on the AC voltage applied using the finite difference method in the generalized coordinate system. In this simulation, the pin-hole leak phenomenon was numerically reproduced by constructing a roller charging system model with photoreceptor defects and its mechanism was clarified. Further, the effects of the BCR (Biased Charging Roller) parameters to reduce the size of the image defect were quantitatively investigated. Consequently, it was suggested that larger BCR resistivity and higher AC frequency were both effective.

## Introduction

Recently, contact chargers<sup>1</sup> have adopted in laser printers and electrophotographic copiers due to low ozone emission and significantly reduced the applied voltage. However, a roller charger, which is one of contact chargers, is known to cause charging troubles when photoreceptor defects such as small scratches or conductive substances exist on a photoreceptor. The photoreceptor defects lead to an insufficient charging, resulting in line or spot type defects appearing in images after the development process. These troubles known as the pin-hole leak phenomenon appear in case of adopting the AC applied voltage and the constant current control, and degree of the defects in images depends on characteristics of rollers.

Several researches have been made to investigate the relations between size of photoreceptor defects and resistance of a BCR (Biased Charging Roller) aiming at reducing the influence of the photoreceptor defects, where a mathematical model was used to solve the static electric field in the photoreceptor and the BCR in contact with each other.<sup>2</sup> As for a numerical scheme for solving a roller charging system, quasi-steady one-dimensional analysis has generally been used. But recently, an unsteady two-dimensional analytical technique, which enables more

detailed analysis considering the effect of components in the circumferencial direction of the rollers, was proposed.<sup>3</sup>

In this study, we proposed a two-dimensional numerical model to reproduce the pin-hole leak phenomenon in the roller charging subsystem, and clarified its mechanism. Moreover, the effects of the BCR parameters to reduce the size of defects in images due to the photoreceptor defects was evaluated.

## Simulation Model

### Basic Equations

The roller charging subsystem is schematically illustrated in Figure 1. Here, the DC voltage superposed on the AC voltage is applied on the BCR, which is in contact with the photoreceptor drum coated by the organic photoconductor (OPC) layer. The OPC surface is charged to the aimed potential after the alternating discharge from the BCR to the OPC and that from the OPC to the BCR by the AC voltage. This subsystem is operated under constant current to assure stable charging performance against environmental variation in BCR parameters such as resistivity.

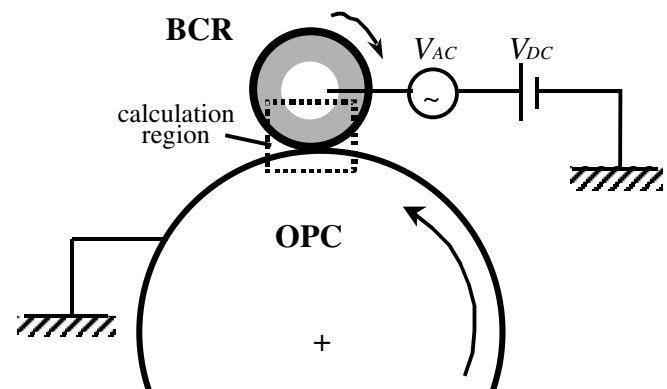


Figure 1. Schematic diagram of the roller charging subsystem with the DC voltage superposed on the AC voltage applied

Basic equations for discharge phenomena in a roller charging subsystem are described as follows:

The Poisson's equation of the electric potential is written as

$$\nabla(\epsilon \nabla \phi) = -q, \quad (1)$$

and the current density conservation equation which expresses flux balance of the charge density in a resistive medium is

$$\frac{\partial q}{\partial t} = \nabla(\sigma \nabla \phi), \quad (2)$$

where  $\phi$  is the potential,  $q$  is the volume charge density,  $\epsilon$  is the permittivity,  $\sigma$  is the conductivity, and  $\nabla$  is the deferential operator.

The rotation of a roller is described using a model that the charge density in a roller moves in the process speed. The advection of the charge density is expressed by the following equation:

$$\frac{\partial q}{\partial t} = \nabla(\mathbf{v} \cdot q), \quad (3)$$

where  $\mathbf{v}$  is the velocity of the rollers.

Discharge is determined by Paschen's law.<sup>4</sup> Paschen's law is used to determine the air discharge along an electric line of force connecting a point on the BCR surface and that on the OPC surface. If the voltage deference between the two points is greater than the Paschen voltage at that point, discharge occurs. Equations described above are discretized by the finite deference method in the generalized coordinate system, and solved using SOR (Successive Over Relaxation) method. In Figure 1, the calculation region is indicated by the area surrounded by the broken line around the nip.

### A Pin-Hole Leak Model

When there is a photoreceptor defect such as a scratch on the surface, the potential at the point where the defect exists becomes close to the grounded voltage. Figure 2 shows a schematic diagram of a photoreceptor defect approaching the nip region. As shown in Figure 2, when a photoreceptor defect enters the discharge area, the pin-hole leak phenomenon occurs in the following mechanism<sup>1</sup>:

1. At the point of a photoreceptor defect, the potential on the OPC surface becomes close to the grounded voltage, and an excessive discharge current flows from the BCR to the photoreceptor defect.
2. Since the system is under the constant current control, applied voltage is reduced to suppress the excessive current.
3. The reduced voltage results in an insufficient charging. After the development process, an image defect such as a black line or a black spot appears around the photoreceptor defect.

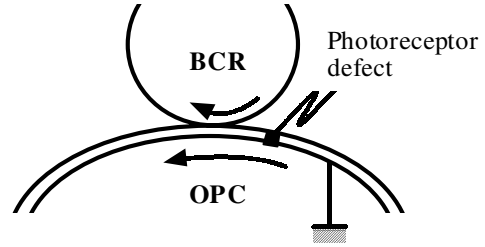


Figure 2. Schematic diagram of a pin-hole leak model

The DC voltage superposed on the AC voltage,  $V_{ap}$ , is described by the formula,

$$V_{ap} = V_{DC} + \frac{1}{2} V_{pp} \sin(2\pi f), \quad (4)$$

where  $V_{DC}$  is the DC applied voltage,  $V_{pp}$  is the peak-to-peak value of the AC applied voltage, and  $f$  is the AC frequency.

Numerically, the constant current control is realized by adjusting the peak-to-peak value of the AC applied voltage,  $V_{pp}$ , to keep the effective value of the total current for each period of the AC applied voltage to the predetermined value. The quantity of the peak-to-peak value of the AC applied voltage to be reduced is determined by applying Ohm's law to the difference between a temporary effective value of the current and predetermined one.

The effect of the photoreceptor defect is considered by locally changing the resistivity of the photoreceptor in the present model. Assuming a scratch on the photoreceptor reaches the grounded base layer where the potential is zero, the resistivity is set low enough to make the potential on the surface zero. In this calculation, as the fixed coordinate system is used, the movement of the photoreceptor defect by the rotation of the OPC drum is expressed by introducing the following simple model:

1. First, set spacing of the calculation grid along the surface of the OPC same as size of the photoreceptor defect, and in each calculation cell between the neighboring two grid points, the resistivity of the OPC is given as an initial value.
2. Based on the rotational angle of the photoreceptor, a calculation cell containing the photoreceptor defect is identified, and the resistivity of that cell is replaced by the value representing the photoreceptor defect.
3. Translate the photoreceptor defect with the process speed for a unit time step in the process direction.
4. Again, identify the cell which contains the photoreceptor defect.

## Numerical Results and Discussion

### Simulation of the Pin-Hole Leak Phenomenon

In this section, results of the calculations for verifying the mechanism of the pin-hole leak phenomenon are presented.

In preliminary calculations, the numerically obtained relationship among the applied voltage, the surface potential and effective value of the current without the photoreceptor defects showed the good agreement with the experimental results.

Figure 3 shows the time sequence of the current,  $I_{ac}$ , as (a) and the applied voltage,  $V_{ap}$ , as (b) in the case where the photoreceptor defects move through the nip. Local distortions near the maximum and the minimum value of the current before 32msec in Figure 3(a) is the consequence of the ordinary discharge. But after 32msec, spike-like peaks appear due to the excessive discharge current. Meanwhile, in Figure 3 (b), reduction of the peak-to-peak value of the AC applied voltage to suppress the excessive current is shown.

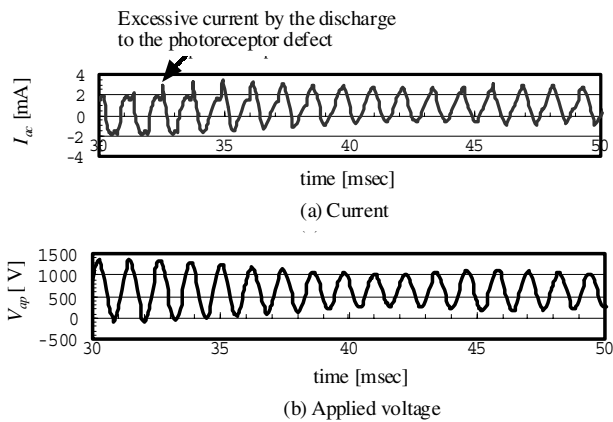


Figure 3. Time sequence of the current and the applied voltage with the photoreceptor defect

Figure 4 represents the time sequence of the effective value of the current,  $I_e$ , and the peak-to-peak value of the AC applied voltage,  $V_{pp}$ . As mentioned above, the peak-to-peak value of the AC applied voltage decreases while the effective value of the current rises due to the effect of the photoreceptor defect. This figure shows that, around 47msec, since the photoreceptor defect is in the nip or close to the nip, the peak-to-peak value of the AC applied voltage falls down to the value lower than a half of the initial one. By the preliminary calculation, the peak-to-peak value of the AC applied voltage under approximately 1.1kV causes an insufficient charging. The small recover of the peak-to-peak value occurring around 45msec is because of that the excessive discharge current decreases near the nip according to Paschen's law since the air gap around the photoreceptor defect becomes very small. The drop in the peak-to-peak value of the AC applied voltage that causes the insufficient charging is recovered by 59msec, where no more discharge to the defect occurs.

Figure 5 illustrates a distribution of the electric potential as (a) and that of the surface potential,  $V_{opc}$ , as (b) at 59msec. In Figure 5(a), the distribution of the electric potential in the air gap is drawn by gray scale, and the

position of the photoreceptor defect is also indicated. Scale of Figure 5(a) in the horizontal direction is same as that of Figure 5(b).

Figure 5(b) shows that an insufficient charging appears for much wider region than the size of the photoreceptor defect. Suppose the development bias is  $V_B$ , which is drawn by the dotted line in Figure 5(b), the region with lower voltage than  $V_B$  is to be unconditionally developed. As a result, the image defect region indicated by the arrow line in Figure 5(a) appears after the development process.

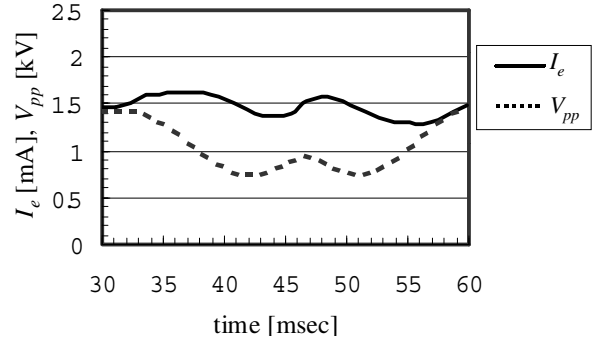


Figure 4. Time sequence of the effective value of the current and the peak-to-peak value of the AC applied voltage

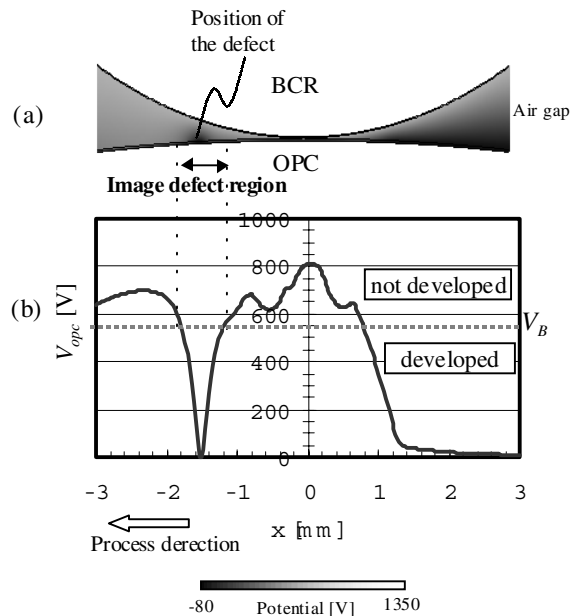


Figure 5. Distribution of (a) the electric potential and (b) the surface potential after the discharge (time=59 msec). Arrow line indicates the image defect region after the development.

**Effects of the BCR Parameters**

In this section, relationship between the image trouble due to the photoreceptor defect and the BCR parameters are investigated, and the effects of the BCR parameters on

reduction of the image defect is evaluated. To reduce the image defect, drop of the peak-to-peak value of the AC applied voltage by the influence of the photoreceptor defect has to be avoided. Therefore, the BCR resistivity and the AC frequency were chosen as the parameters to be investigated because of the following reasons:

1. Increase of the BCR resistivity tends to suppress the current even in the case that the discharge to the photoreceptor defect occurs.
2. The high frequency of the AC applied voltage shortens the interval of voltage correction for constant current control.

Note that other effects producing image defects such as the moire pattern by the AC frequency is not considered, and that the initial value of the applied voltage is equal for all BCR parameters here.

Figure 6 indicates the relationship between the BCR resistivity and the size of the image defect. This result shows that high resistivity appears to be effective to decrease the size of the image defect. However, Figure 6 also suggests that there is a limitation of the improvement. Here, the range of the resistivity that causes an insufficient charging even without a photoreceptor defect was not considered.

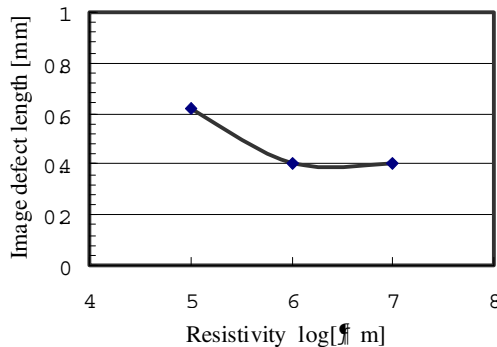


Figure 6. Relationship between the image defect length and the resistivity of the BCR

Figure 7 demonstrates the relation between the AC frequency and the size of the image defect. Here, the BCR resistivity is set to  $5 \log \Omega m$ . In Figure 7, it can be seen that setting the AC frequency higher is effective to reduce the size of the image defect. However, it suggests that, like the case in Figure 6, there is a limit for the improvement.

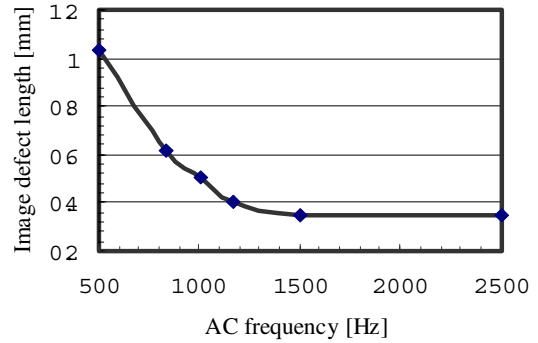


Figure 7. Relationship between the image defect length and the AC frequency

## Conclusion

In this study, a problem in the BCR charger known as the pin-hole leak phenomenon was reproduced using numerical simulation in two-dimensional space, and the mechanism that causes the insufficient charging due to a photoreceptor defect was clarified in detail. Further, the effects of the BCR parameters on the size of the image defect were investigated. Consequently, it was suggested that larger BCR resistivity and higher AC frequency were both effective to reduce the size of the image defect.

## References

1. Nakamura, J. *Electrophotography Soc. of Jpn.*, **3**, 30 (1991).
2. H. Kawamoto and H. Satoh, *J. Imaging. Sci. and Technol.*, **4**, 38 (1994).
3. M. Kadonaga, *J. Imaging Soc. of Jpn.*, **2**, 38(1999).
4. T. Ito and H. Kawamoto, *Proc. The 10th International Symposium on Applied Electromagnetics and Mechanics*, pg. 49. (2001).

## Biography

Satoshi Hasebe received his B.S. degree in Mechanical Engineering from Hokkaido University in 1991 and a Doctor Degree in 1997. He primarily studied on the computational fluid dynamics. Since 1997 he has joined at Fuji Xerox Co., Ltd., and now works in the Document Products Company Research and Development Center of Fuji Xerox. His work is primarily focused on modeling and numerical simulation of the sub processes in the electrophotography, especially the charging process, and also focused on a development of numerical techniques for them.